The Astrophysical Journal, 501:L17–L20, 1998 July 1

THE TeV SPECTRUM OF MARKARIAN 501

F. W. Samuelson,[1] S. D. Biller,[2] I. H. Bond,[3] P. J. Boyle,[4] S. M. Bradbury,[3] A. Breslin,[3] J. H. Buckley,[5] A. M. Burdett,[3] J. Bussóns Gordo,[4] D. A. Carter-Lewis,[1] M. Catanese,[1] M. F. Cawley,[6] D. J. Fegan,[4] J. P. Finley,[7] J. A. Gaidos,[7] T. Hall,[7] A. M. Hillas,[3] F. Krennrich,[1] R. C. Lamb,[8] R. W. Lessard,[7] J. E. McEnery,[9] C. Masterson,[4] J. Quinn,[10] A. J. Rodgers,[3] H. J. Rose,[3] G. H. Sembroski,[7] R. Srinivasan,[7] V. V. Vassiliev,[10] T. C. Weekes,[10] and J. Zweerink[11]
Received 1998 March 26; accepted 1998 May 5; published 1998 June 18

ABSTRACT

The energy spectrum of the active galactic nucleus Markarian 501 has been determined from 0.3 to 10 TeV with the Whipple Observatory Cerenkov Imaging Telescope, by using both small zenith angle and large zenith angle data taken between 1997 February 14 and June 8. The TeV emission from Mrk 501 was unprecedentedly high, allowing a statistically accurate spectrum to be derived. In contrast to previously measured TeV spectra, the spectrum over this energy region is not well described by a simple power law. Instead, the spectrum exhibits significant curvature and can be well fitted by a parabolic spectrum proportional to $E^{-2.22\pm0.04\pm0.05-(0.47\pm0.07)\log_{10}E}$, where the first set of errors is statistical and the second systematic and E is in units of TeV. Simple power-law fits to the TeV data are also inconsistent with upper limits from EGRET observations that temporally overlap a subset of the TeV observations. The data show a statistically significant signal above energies of 7 TeV. This energy, combined with variability timescales, yields a Doppler beaming factor, δ, of at least 1.5.

Subject headings: BL Lacertae objects: individual (Markarian 501) — gamma rays: observations

1. INTRODUCTION

Within the last few years, three TeV-emitting active galactic nuclei (AGNs) have been discovered. These are Markarian 421 (Punch et al. 1992), Markarian 501 (Quinn et al. 1996), and 1ES 2344+514 (Catanese et al. 1998). All three are BL Lacertae (BL Lac) objects, members of the blazar class of AGNs that are believed to have relativistic beams pointed very nearly in the direction of Earth. Since their discovery, multiwavelength observations have shown that the overall spectra of Mrk 421 and Mrk 501 are roughly consistent with a two-component picture: a low-energy part extending as high as 100 keV, which is believed to be synchrotron emission from highly relativistic electrons, and a high-energy part that extends up to the TeV regime. The higher energy component is usually attributed to inverse Compton scattering of IR/visible photons by the same highly relativistic electrons that produce the synchrotron emission (e.g., Maraschi, Ghisellini, & Celotti 1992; Ghisellini, Maraschi, & Dondi 1996; Marscher & Travis 1996), although gamma-ray emission from π^0s produced by a hadronic component in the relativistic beam is not ruled out (e.g., Mannheim 1993). The TeV emission from the detected BL Lac objects is extremely variable, exhibiting dramatic flares on timescales as short as 15 minutes (Gaidos et al. 1996) and flux amplitude variations of up to a factor of 100.

Energy spectra in the TeV range have been published previously for Mrk 421 (Zweerink et al. 1997) and Mrk 501 (Bradbury et al. 1997; Aharonian et al. 1997). These are consistent with a simple power law, $J(E) \sim E^{-\gamma}$, where $J(E)$ is the differential flux and the measured values of γ are $2.56 \pm 0.07 \pm 0.10$ (statistical and systematic errors, respectively) for Mrk 421 and 2.49 ± 0.11 (statistical error only) for Mrk 501. The general power-law spectral shape may reflect power-law–shaped spectra of the primary ultrarelativistic electrons or protons, perhaps arising from shock acceleration. On the other hand, even with a simple power-law primary spectrum, some curvature is expected from the inverse Compton mechanism (Hillas 1998). Moreover, this high-energy component of the gamma-ray spectrum must drop below a simple power-law extrapolation as one moves toward lower energies in order to be consistent with the weak detections/upper limits of the three TeV-emitting AGNs at GeV energies obtained by the Energetic Gamma-Ray Experiment Telescope (EGRET) instrument on the *Compton Gamma Ray Observatory* (*CGRO*) (Fichtel et al. 1994; D. Macomb 1998, private communication).

Similarly, at higher energies it is anticipated that absorption from photon-photon scattering with the infrared intergalactic background radiation will cause the observed spectrum to drop below a simple power-law extrapolation (Gould & Schréder 1967; Stecker & de Jager 1993). This opacity rises with energy and is possibly one of the important factors limiting the number of AGNs that have been detected at TeV energies (three) compared with GeV energies (about 60). A maximum energy in the accelerated particles, be they electrons or protons, is a second mechanism by which the TeV gamma-ray flux from an AGN may drop below a simple power-law extrapolation. Models in which gamma rays are produced from relativistic protons in the AGN beam generally predict higher endpoint energies

[1] Department of Physics and Astronomy, Iowa State University, Ames, IA 50011-3160; dalewis@iastate.edu.
[2] Department of Physics, Oxford University, Oxford, England, UK.
[3] Department of Physics, University of Leeds, Leeds, LS2 9JT, Yorkshire, England, UK.
[4] Experimental Physics Department, University College, Belfield, Dublin 4, Ireland.
[5] Department of Physics, Washington University, St. Louis, MO 63130.
[6] Physics Department, St. Patrick's College, Maynooth, County Kildare, Ireland.
[7] Department of Physics, Purdue University, West Lafayette, IN 47907.
[8] Space Radiation Laboratory, California Institute of Technology, Pasadena, CA 91125.
[9] Present address: Department of Physics, University of Utah, Salt Lake City, UT 84112.
[10] Fred Lawrence Whipple Observatory, Harvard-Smithsonian Center for Astrophysics, P. O. Box 97, Amado, AZ 85645-0097.
[11] Loras College, Dubuque, IA 52004.

than electron models (e.g., Sikora 1994). In order to distinguish the effects of these mechanisms and to confirm or reject the corresponding models, wide-ranging, detailed spectra are necessary, ideally for many objects.

In this Letter, we present the results from Cerenkov imaging gamma-ray observations of Mrk 501 taken in 1997 with the 10 m Whipple Observatory telescope, which show a detailed TeV spectrum from 0.3 to 10 TeV. We were able to extend spectral measurements to higher energies by (1) using a new camera with a wider field of view (Weekes et al. 1997), which gave better energy estimates for high-energy events, and (2) using large zenith angle observations (Krennrich et al. 1997), for which the collection area is much larger at higher energies. We were also fortunate to have observations during which Mrk 501 was particularly active; i.e., the flux was about a factor of 8 higher than the average flux measured in 1996 (Quinn et al. 1998). The spectrum is not statistically consistent with a simple power law but is well fitted if a single curvature parameter is included. The highest estimated energy above which a statistically significant (3 σ) signal was found is 8 TeV. With detector resolution effects incorporated, we can state that primary photon energies above 7 TeV were present in the signal at the 95% confidence level. We see no evidence for temporal variability of the spectral shape within the data set.

2. OBSERVATIONS

The observations reported here were made with the Whipple Observatory Cerenkov Imaging Telescope (Cawley et al. 1990), which consists of a 10 m reflector focusing onto a photomultiplier tube camera. The camera had been upgraded in late 1996 from 109 to 151 pixels, which were placed on a $\frac{1}{4}$ degree hexagonal matrix covering a field of view with a 3°.2 diameter. The camera was triggered by Cerenkov light from air showers when two of the inner 91 photomultiplier tubes exceeded a threshold of ∼50 photoelectrons each within a time window of ∼15 ns, and the light striking each tube was digitized. The focal plane images were used to distinguish gamma-ray–initiated showers from those from initiated by hadrons and to estimate the energies of the primary gamma rays as described in § 3.

The field of view of the 151 pixel camera was larger than that of previous (109 pixel) cameras (3°.2 vs. 2°.7). This is useful for energy spectra measurement, particularly at large energies, ∼10 TeV near the zenith. At energies of about 10 TeV, parts of the images fell outside of the field of view of the 109 pixel camera, making energy estimation difficult, as described in Mohanty et al. (1998). With the new camera, we were able to measure spectra for energies to about 10 TeV by using the standard observing and analysis methods.

The data consist of pairs of observations in which the telescope is pointed at Mrk 501 for 28 minutes and then at a background region of the sky for 28 minutes, spanning the same range of elevation and azimuth angles. At small zenith angles, the telescope energy threshold is lowest; hence, the counting rate is highest. At large zenith angles, the energy threshold is high, but so is the collection area (see below). Observations of Mrk 501 near the zenith were made with the 151 pixel camera from February 14 to June 8, for a total of 16 hr of on-source data, with the same time spent off-source. The Crab Nebula serves as a standard candle for TeV gamma rays. Consequently, observations of the Crab with the 151 tube camera made in 1997 January and February provide a check of spectra extracted with the new camera.

In addition to small zenith angle (8°–25°) observations, we also present data measured at large zenith angles (55°–60°). At these large angles, both the maximum collection area and the threshold energy are significantly increased, making it an effective method for measuring the upper end of the energy spectrum. A total of 5.1 hr of large zenith angle data were measured on-source, with an equivalent amount of off-source observations. The details of the method and the measurements for the standard candle, the Crab Nebula, are given in another paper (Krennrich et al. 1998). Here we present high-energy large zenith angle data that overlap the spectrum obtained with our standard observing procedure to confirm our results.

3. ANALYSIS AND RESULTS

Our techniques for determining TeV spectra are described by method 1 of Mohanty et al. (1998). Very briefly, the analysis proceeds as follows. Selection criteria (extended supercuts) derived from simulations were used to differentiate gamma-ray images from cosmic-ray images. Then an energy based on the total image light and image centroid location was estimated for each event, and the estimated energies for both on-source and off-source data were histogrammed. The differences in the histograms were ascribed to gamma rays from Mrk 501, and the telescope resolution and collection area were then incorporated to extract spectra. A comparison between the real excess and simulated total light distributions using a nonparametric order statistic and different selection criteria yields similar results.

For a Cerenkov telescope, the threshold is defined as the energy at which the gamma-ray count rate is at a maximum for a differential spectrum with an index of −2.7 (Weekes 1976). It is discussed, along with collection area and energy resolution, in Mohanty et al. (1998). For the small zenith angle data discussed here, the energy threshold was ∼0.5 TeV, the maximum collection area was $\sim 6.5 \times 10^8$ cm^2, and the resolution function rms deviation was $\Delta E/E \sim 0.36$. For the large zenith angle data, the energy threshold was ∼1.1 TeV, the maximum collection area was $\sim 13 \times 10^8$ cm^2, and the resolution function rms deviation was $\Delta E/E \sim 0.29$ (Krennrich et al. 1998).

We have monitored the Crab Nebula with a 109 pixel or larger camera since 1989. The data show no evidence of either flux or spectral index variability (Mohanty 1995; Cawley et al. 1998). Using exactly the same analysis techniques as that used for Mrk 501, we reanalyzed the 1989, 1995, and 1997 Crab databases. The 1997 Crab database was measured with the same camera as that used for the Mrk 501 observations. Both large zenith angle and small zenith angle data from 1997 Crab observations gave a simple power law that is consistent with our standard Crab spectrum (Hillas et al. 1998) over the respective energy ranges. However, as pointed out in this latter reference, the Crab spectrum must drop below a simple power-law extrapolation to be consistent with EGRET data, and an alternative fit including curvature is also given. With the TeV data alone, both single power-law and curvature fits are acceptable.

Observations of Mrk 501 from the 1997 observing season showed a flux ranging from 1.0 to 4.1 times that of the Crab Nebula, with an average flux of 1.6 Crab units. The TeV spectrum from the entire 1997 season is shown in Figure 1. Because of the finite resolution of the telescope, the energies, E, are actually estimated energies. The fluxes have been multiplied by E^2, making it effectively a νF_ν plot, which used in other energy regimes. The crosses indicate data from observations

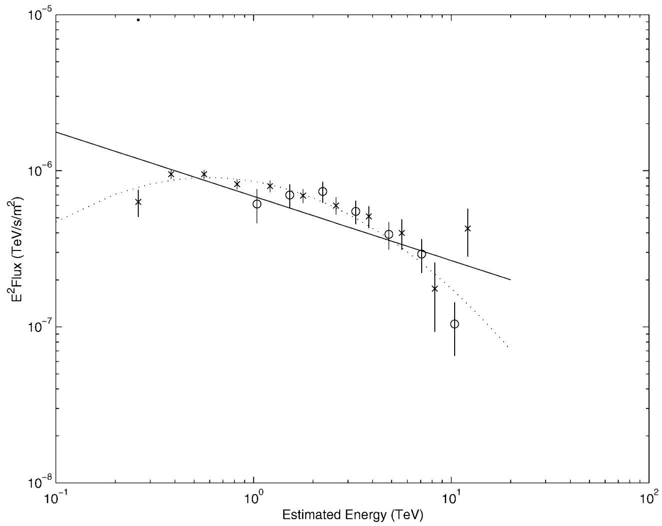

FIG. 1.—The TeV spectrum of Mrk 501. The data measured near the zenith are indicated by the crosses, and the data measured at large zenith angles are indicated by the open circles. The relative normalization between the two data sets has been adjusted because Mrk 501 is variable and the observations are not contemporaneous. The solid line is fitted assuming a simple power-law form, yielding $\chi^2 = 59.7$ with 15 degrees of freedom (chance probability of 2.8×10^{-7}). The dotted line includes a curvature term (i.e., is parabolic on a log-log plot), which gives $\chi^2 = 17.1$ with 14 degrees of freedom (chance probability of 0.25).

near the zenith, and the open circles are data from large zenith angles. Although the large zenith angle data comprise a smaller data set (5 hr of observations at large zenith angles vs. 16 hr at small zenith angles), the statistical accuracy is roughly comparable at energies near 10 TeV because of the larger effective area of the large zenith angle technique (Krennrich et al. 1998). Because Mrk 501 is variable, and the telescope has much different high-energy versus low-energy sensitivity at large/small zenith angles, the overall normalization of the large zenith angle data was adjusted to match the small zenith angle data as described below.

We first fit *only* the small zenith angle data with a simple power law, which yields

$$J(E) = 7.4 \times 10^{-7}\left(\frac{E}{1\ \mathrm{TeV}}\right)^{-2.27 \pm 0.04}$$

photons $\mathrm{m}^{-2}\ \mathrm{s}^{-1}$ with $\chi^2 = 26.9$ for 9 degrees of freedom, giving a chance probability of 0.00145. Thus, there is evidence for curvature from these data alone. A power-law fit to the large zenith angle data yields

$$J(E) = 7.5 \times 10^{-7}\left(\frac{E}{1\ \mathrm{TeV}}\right)^{-2.67 \pm 0.09}$$

photons $\mathrm{m}^{-2}\ \mathrm{s}^{-1}$ with $\chi^2 = 14.8$ for 5 degrees of freedom, giving a chance probability of 0.01. We next analyzed the data sets together with the normalization of the large zenith angle data taken as an additional free parameter in the minimization of χ^2. This resulted in the two curves shown in Figure 1. The solid straight line is a simple power law that yields $\chi^2 =$ 59.7 with 15 degrees of freedom (chance probability of 2.8×10^{-7}), and the dashed line includes a curvature term that yields $\chi^2 = 17.1$ with 14 degrees of freedom (chance probability of 0.25). The simple power-law fit has the form

$$J(E) = 7.3 \times 10^{-7}\left(\frac{E}{1\ \mathrm{TeV}}\right)^{-2.32 \pm 0.027}$$

photons $\mathrm{m}^{-2}\ \mathrm{s}^{-1}$, and the curvature fit is

$$J(E) = (8.6 \pm 0.3 \pm 0.7) \times 10^{-7} \times \left(\frac{E}{1\ \mathrm{TeV}}\right)^{-2.20 \pm 0.04 \pm 0.05 - (0.45 \pm 0.07)\log_{10} E}$$

photons $\mathrm{m}^{-2}\ \mathrm{s}^{-1}$ (the first set of errors are statistical and the second are estimates of systematic errors as described in Mohanty et al. 1998; the systematic errors in the $\log_{10} E$ coefficient are estimated to be small compared with the statistical errors). We note that although the highest energy point in the small zenith angle data appears high to the eye, it is less than 2 σ above the fit curve. We did examine the data for this point and found no reason to reject it. (There are 18 data points in the spectrum, and the overall χ^2 is reasonable.) In conclusion, with the combined data sets, the evidence for curvature is statistically compelling.

In order to estimate the maximum energy present in the signal, we first applied a simple energy cutoff to the data and found a 3 σ excess for energies above 8 TeV. However, because of the finite resolution of the telescope, this is an estimated energy, not a real energy. We obtained a more rigorous limit by simulating data for which the flux falls sharply to zero above a cutoff energy, E_c, and calculating χ^2 for the points in the spectrum above E_c. This leads to a minimum energy in the signal of 7 TeV at the 95% confidence level; i.e., no sudden cutoff appears before 7 TeV at a 95% confidence level. There is also an overall uncertainty in the energy scale of about 16% (see Mohanty et al. 1998).

Parts of the Mrk 501 observations were taken contemporaneously with EGRET observations at GeV energies (1997 April 9–15). Thus, the EGRET upper limits (D. Macomb 1998, private communication) can be meaningfully compared with this limited set of TeV data (3 hr total on-source). These are shown in Figure 2, in which the vertical axis is multiplied by E^2, as was done in Figure 1. Clearly the simple power law cannot extend without change to GeV energies, but the curvature fit is consistent with the EGRET results.

4. DISCUSSION

We have derived the spectrum of Mrk 501 from the 1997 Whipple Observatory data spanning the range 0.3–10 TeV. The data are not statistically consistent with a single power law, but they are consistent with a simple generalization that includes a curvature term. At lower energies, the curvature must occur to be consistent with upper limits at EGRET energies. Possible causes of curvature at higher energies include partial absorption of the gamma rays in the intergalactic medium, absorption in the jet by pair production on low-energy photons, absorption by photons near the source (Dermer & Schlickeiser 1994), or an end in the primary particle beam energy. The first of these has been advocated by a number of authors (Stecker & de Jager 1993; Dwek & Slavin 1994; de Jager, Stecker, & Salamon 1994; Biller et al. 1995) as a potential cause of such

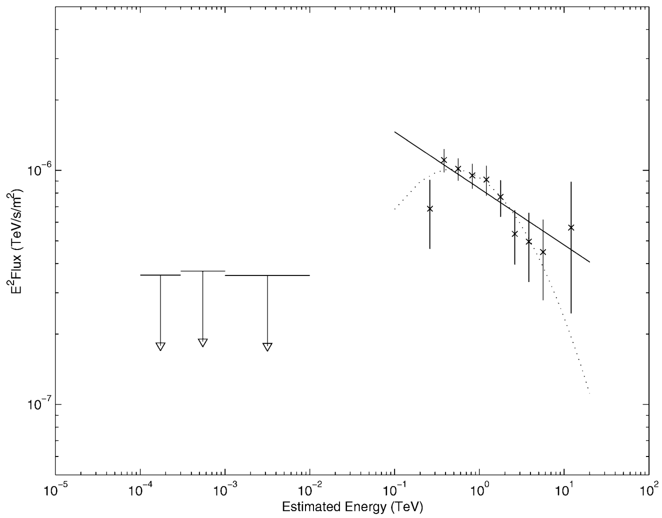

FIG. 2.—Upper limits for Mrk 501 from the EGRET detector compared with spectra from roughly contemporaneous TeV observations. The TeV data used in this figure comprise only 3 hr on-source and are only a small subset of the data for the season. The simple power-law (*solid line*) and curvature (*dotted line*) fits are shown. It is clear from the figure that, over this wider range, a simple power law is not consistent with the EGRET limits, whereas the curvature fit is.

effects, and it is possible that the form of the spectrum might be modified to some extent by such absorption. By considering the extent of this potential modification to AGN spectra, upper limits to the density of the extragalactic IR field (yet to be detected) may thus be determined. Such limits have recently been set (Biller et al. 1998) in a fairly robust manner using data from Mrk 421 (Zweerink et al. 1997) together with earlier data from Mrk 501 (Aharonian et al. 1997). Similar limits were also derived by Stanev & Franceschini (1997) from the earlier Mrk 501 data. While the Mrk 501 data presented here represent more detail than was previously available owing to better statistics, the extent and shape of this spectrum are still reasonably accommodated within the assumptions made by Biller et al. (1998). Hence, these limits are negligibly affected by the data presented here. Nevertheless, the data may still provide constraints on models that incorporate detailed shapes for intergalactic IR photon spectra and AGN gamma-ray spectra. In the future, the IR limits may be improved on either by establishing that emission continues to even higher energies and/or by observing TeV emission from sources at farther redshifts. Indeed, the fact that there is as yet no clear evidence for substantial IR absorption taking place at energies as high as 10 TeV or more for emission from Mrk 501 indicates that more distant sources should be visible to TeV gamma-ray telescopes.

The extension of the gamma-ray spectrum to multi-TeV energies and correlations between the TeV gamma rays and X-rays (Catanese et al. 1997) allow a limit to be set on the Doppler factor of the jet in Mrk 501. As derived in Catanese et al. (1997), if it is assumed that the gamma-ray emission derives from inverse Compton scattering by the same electrons that produce the synchrotron emission, an inequality for the magnetic field, B, is implied:

$$(E_{\rm obs}\delta\Delta t_{\rm obs}^2)^{-1/3} \lesssim B \lesssim 2E_{\rm syn}\delta/E_{\rm C}^2, \tag{1}$$

where $E_{\rm obs}$ is the energy in units of eV of the observed synchrotron variability, $\Delta t_{\rm obs}$ is timescale of the synchrotron variability in units of days, δ is the Doppler factor of the jet, B is in units of Gauss, $E_{\rm syn}$ is the location of the synchrotron cutoff in units of 100 keV, and $E_{\rm C}$ is the maximum inverse Compton energy. If this inequality is not satisfied, Doppler beaming is implied. For the observed 1 day correlated variability between the *Rossi X-Ray Timing Explorer* All-Sky Monitor at $E_{\rm obs} = 2000$ eV and TeV gamma rays and the synchrotron emission extent of $E_{\rm syn} \gtrsim 100$ keV measured by the Oriented Scintillation Spectrometer Experiment (OSSE) on *CGRO*, and the result presented here that $E_{\rm C} \gtrsim 7$ TeV, equation (1) is not satisfied and a Doppler limit of $\delta \gtrsim 1.5$ is implied. While this is not as high as the limits derived previously from Mrk 421 (Gaidos et al. 1996; Buckley et al. 1997), it is the first evidence of relativistic beaming of the gamma-ray emission in Mrk 501, although again it assumes that the gamma-ray emission is the result of inverse Compton scattering of electrons.

We gratefully acknowledge the assistance of Patrick Moriarty and Kevin Harris and thank Daryl Macomb for providing the EGRET upper limits. This research is supported by grants from the U.S. Department of Energy and by NASA, by PPARC in the UK, and by Forbairt in Ireland.

REFERENCES

Aharonian, F., et al. 1997, A&A, 327, L5
Biller, S. D., et al. 1995, ApJ, 445, 227
———. 1998, Phys. Rev. Lett., in press
Bradbury, S. M., et al. 1997, A&A, 320, L5
Buckley, J. H., et al. 1997, in AIP Conf. Proc. 410, Proc. Fourth Compton Symp., ed. C. D. Dermer, M. S. Strickman, & J. D. Kurfess (New York: AIP), 1381
Catanese, M., et al. 1997, ApJ, 487, L143
———. 1998, ApJ, in press
Cawley, M. F., Fegan, D. J., Harris, K., Kwok, P. W., & Hillas, A. M. 1990, Exp. Astron., 1, 173
Cawley, M. F., et al. 1998, ApJ, in preparation
de Jager, O. C., Stecker, F. W., & Salamon, M. H. 1994, Nature, 369, 294
Dermer, C. D., & Schlickeiser, R. 1994, ApJS, 90, 945
Dwek, E., & Slavin, J. 1994, ApJ, 436, 696
Fichtel, C. E., et al. 1994, ApJS, 94, 551
Gaidos, J. A., et al. 1996, Nature, 383, 319
Ghisellini, G., Maraschi, L., & Dondi, L. 1996, A&AS, 120, 503
Gould, R. P., & Schréder, G. P. 1967, Phys. Rev., 155, 1408
Hillas, A. M. 1998, in preparation
Hillas, A. M., et al. 1998, ApJ, in press
Krennrich, F., et al. 1997, ApJ, 481, 758
———. 1998, in preparation
Mannheim, K. 1993, A&A, 269, 67
Maraschi, L., Ghisellini, G., & Celotti, A. 1992, ApJ, 397, L5
Marscher, A. P., & Travis, J. P. 1996, A&AS, 120, 537
Mohanty, G. 1995, Ph.D. thesis, Iowa State Univ.
Mohanty, G., et al. 1998, Astropart. Phys., in press
Punch, M., et al. 1992, Nature, 358, 477
Quinn, J., et al. 1996, ApJ, 456, L83
———. 1998, in preparation
Sikora, M. 1994, ApJS, 90, 923
Stanev, T., & Franceschini, A. 1997, ApJ, submitted
Stecker, F. W., & de Jager, O. C. 1993, ApJ, 415, L71
Weekes, T. C. 1976, Nuovo Cimento, 25B, 95
Weekes, T. C., et al. 1997, Towards a Major Atomospheric Cerenkov Detector–V, ed. O. C. de Jager (Potchefstroom: Wesprint), 202
Zweerink, J. A., et al. 1997, ApJ, 490, L141